OPEN

Personalized Chest Computed Tomography
Minimum Diagnostic Radiation Dose Levels for the Detection of Fibrosis, Nodules, and Pneumonia

Matthias May, MD,* Rafael Heiss, MD,* Julia Koehnen, MD,* Matthias Wetzl, MD,*
Marco Wiesmueller, MD,* Christoph Treutlein, MD,* Lars Braeuer, MD,†
Michael Uder, MD,* and Markus Kopp, MD*

Objectives: The purpose of this study was to evaluate the minimum diagnostic radiation dose level for the detection of high-resolution (HR) lung structures, pulmonary nodules (PNs), and infectious diseases (IDs).

Materials and Methods: A preclinical chest computed tomography (CT) trial was performed with a human cadaver without known lung disease with incremental radiation dose using tin filter-based spectral shaping protocols. A subset of protocols for full diagnostic evaluation of HR, PN, and ID structures was translated to clinical routine. Also, a minimum diagnostic radiation dose protocol was defined (MIN). These protocols were prospectively applied over 5 months in the clinical routine under consideration of the individual clinical indication. We compared radiation dose parameters, objective and subjective image quality (IQ).

Results: The HR protocol was performed in 38 patients (43%), PN in 21 patients (24%), ID in 20 patients (23%), and MIN in 9 patients (10%). Radiation dose differed significantly among HR, PN, and ID (5.4, 1.2, and 0.6 mGy, respectively; $P < 0.001$). Differences between ID and MIN (0.2 mGy) were not significant ($P = 0.262$). Dose-normalized contrast-to-noise ratio was comparable among all groups ($P = 0.087$). Overall IQ was perfect for the HR protocol (median, 5.0) and decreased for PN (4.5), ID-CT (4.3), and MIN-CT (2.5). The delineation of disease-specific findings was high in all dedicated protocols (HR, 5.0; PN, 5.0; ID, 4.5). The MIN protocol had borderline IQ for PN and ID lesions but was insufficient for HR structures. The dose reductions were 78% (PN), 89% (ID), and 97% (MIN) compared with the HR protocols.

Conclusions: Personalized chest CT tailored to the clinical indications leads to substantial dose reduction without reducing interpretability. More than 50% of patients can benefit from such individual adaptation in a clinical routine setting. Personalized radiation dose adjustments with validated diagnostic IQ are especially preferable for evaluating ID and PN lesions.

Key Words: personalized medicine, chest CT, CT, pneumonia, ultra–low-dose CT, radiation dose reduction, lung cancer screening

C ontemporary computed tomography (CT) of the chest is widespread and plays a crucial role in the health care systems, especially during the coronavirus (SARS-CoV-2) pandemic.[1–3] Continuous technical developments increased the dose efficiency of CT scanners. Improved detector technology with high photon efficiency can decrease the radiation dose by 60% to 80%.[4] Moreover, spectral shaping of the x-ray beam by tin prefiltration can minimize the radiation dose below the conventional limits and increase spatial resolution.[5,6] The lowest submillisievert dose levels, comparable to radiographs in 2 planes, are possible using these techniques.[7] Saltybaeva et al[8] were able to prove that these protocols[9] can also substantially reduce the risk for de novo induction of lung cancer to 0.35 per 100,000 cases, which is especially important for repetitive examinations in large patient collectives. Delineation of pulmonary structures generally seems more resistant to radiation dose reduction than mediastinal structures.[10] Therefore, lung cancer screening is a particular focus for low-dose CT of the chest. Several studies provided promising results concerning sensitivity and specificity for pulmonary nodule (PN) detection.[11–14] The National Lung Screening Trial proved reduced mortality for US patients that undergo screening examinations at 1.5 mSv but limited the evaluation to lesions larger than 4 mm.[15] Other studies reported detection rates of approximately 90% for nodules larger than 5 mm in intraindividual double exposure study designs, comparing 0.13 to 1.8 mSv.[16] The only study comparing more than 2 radiation dose settings in a triple exposure study design found that 0.14 mSv examinations provide significantly reduced image quality (IQ) compared with 0.96 and 3.3 mSv, especially for subsolid lesions and lesions below 4 mm in obese patients.[17] They, therefore, concluded that the radiation dose should be tailored to each individual patient and each indication.

Different studies evaluated low-dose protocols at a single radiation dose setting for diverse clinical tasks and personal situations. Xu et al[18] found a good representation of interstitial lung disease, except for peripheral bronchi, vessels, and reticulations, in patients with connective tissue disease at 0.3 mSv. Cystic fibrosis was successfully evaluated in inspiration at 0.69 mSv and in expiration at 0.35 mSv by Loeve et al.[19] Only a few authors evaluated inflammatory lung disease in a low-dose setting, but Wendel et al[20] suggested 0.6 mSv to obtain high sensitivity and specificity. Most recently, a protocol with 0.28 mSv was proposed for diagnostic workup of coronavirus disease (COVID-19).[21]

This study aims to prospectively evaluate the performance of personalized radiation dose protocols adapted to the clinical indication. The null hypothesis was defined as decreased IQ with reduced radiation doses. The alternative hypothesis follows a noninferiority approach for different pathologic lesions at different radiation dose levels.[8,16,22,23]

MATERIALS AND METHODS

Ex-Ante Trial

A recent male human cadaver with a representative body constitution (approximately 180 cm height and 70 kg body weight) was used for an ex-ante trial. The time of death was within the last 24 hours to maintain the lung ventilation to some extent comparable to in vivo scans. There were no lung pathologies known in the medical recordings. We used an existing institutional examination protocol from our clinical routine to detect relevant lung structures with upper dose reference protocol

TABLE 1. Protocol Parameters and Radiation Dose Levels for Ex-Ante Human Cadaver Examinations

Scan	kV	eff mAs/ref mAs	CTDI$_{vol}$, mGy	DLP, mGy · cm	ED, mSv
#1 lower reference	110	6/1	0.42	12	0.17
#2 lower reference	80	6/1	0.16	4	0.06
#3 lower reference	Sn 110	5/1	0.07	2	0.03
#4	Sn 110	7/10	0.11	3	0.04
#5 (MIN-CT)	Sn 110	14/20	0.21	6	0.08
#6	Sn 110	30/40	0.43	12	0.17
#7 (ID-CT)	Sn 110	61/80	0.87	24	0.34
#8 (PN-CT)	Sn 110	119/160	1.71	46	0.64
#9	Sn 110	227/320	3.24	85	1.19
#10 upper reference (HR-CT)	110 kV	136/130	7.15	300	4.2

Reference mAs were exponentially increased between the lower and upper reference protocol (protocol #1–3 and #10). Radiation dose was assessed as CTDI$_{vol}$, DLP, and ED. Protocol #1 to 9 were performed on the single-source trial scanner. Upper reference protocol #10 was performed on the reference dual-source scanner with dose settings from the clinical routine. The K-factor for the calculation of ED was 0.014.

ref mAs, reference mAs; CTDI$_{vol}$, volumetric CT dose index; DLP, dose length product; ED, effective dose.

settings and IQ (110 kV; 130 mAs reference current-time product; volumetric CT dose index [CTDI$_{vol}$], 7.15 mGy) (SOMATOM Force; Siemens Healthcare GmbH, Forchheim, Germany). The trial was performed using a modern single-source volume CT (SOMATOM go.Up; Siemens Healthcare GmbH, Forchheim, Germany). We decided to use the factory protocol for full-dose high-resolution (HR) CT (130 kV, 54 reference mAs [ref mAs]) as recommended by the vendor. The scanner only has 80, 110, and 130 kV available, and the tube capacity is comparably lower than in a dual-source high-end scanners. Therefore, all study HR examinations were selected by the scanner to be done with 130 kV.

The preclinical part of the study aimed to determine the minimum diagnostic dose levels for chest CT. Effective current-time product were calculated by the scanner using a tube current modulation algorithm (CareDose). No tube voltage adaptation was allowed. In addition to the upper reference protocol, the human cadaver was examined with 9 different low-dose protocols (Table 1). Three different lower reference protocols with reference current-time products of 1 mAs were used (#1, 110 kV; #2, 110 kV with tin prefiltration; #3, 80 kV). Six of those examination protocols were used with tin prefiltration (0.4 mm tin) at a constant tube voltage (110 kV) and exponentially increasing reference

Preclinical image quality assessment for low-dose chest CT with tin (Sn)-prefiltration compared to the full-dose high-resolution (HR)-CT.

	Scan protocol	#1	#2	#3	#4	#5	#6	#7	#8	#9	#10
	Dose length product [mGy]	12	4	2	3	6	12	24	46	85	300
	CNR	19.6	7.3	4.2	4.8	10.5	26.1	29.0	47.3	63.8	80.8
	CNRD	30.4	18.2	15.8	14.4	23.1	39.7	31.1	36.3	35.5	30.2
	[kV]/[ref. mAs]	110/1	80/1	Sn110/1	Sn100/10	Sn110/20	Sn110/40	Sn110/80	Sn110/160	Sn110/320	110/130
	Overall image quality										
		3	2	1	2	3	3	4	4	5	5
	High-resolution structures										
HR structures	Secondary lobules	2	1	1	1	1	2	4	4	5	5
	Intralobular lines	2	1	1	1	1	2	3	3	4	5
	Lung fissures	3	2	2	2	3	4	4.5	5	5	5
	Subpleural curvilinear lines	3	2	1	1	2.5	3.5	4	4	4	5
	Parenchymal bands	3	2	2	2	3	3	4	5	5	5
	Pleural thickening	3	2	2	2	3	4	4	4	5	5
	Bronchioldectasis	2.5	1	1	1	3	3	3	4.5	5	5
	Bullae	3	2	2	2	3	3.5	4	5	5	5
	Centrilobular emphysema	2	2	2	2	2	3	3	3.5	5	5
	Pulmonary nodules										
PN lesions	Granuloma	4	3	3	3	4	4	4.5	5	5	5
	Micronodules < 3mm	3	2	1	2	3	3	3	4	5	5
	Infectious disease lesions										
ID lesions	Consolidations	4	3	2.5	3	4	4	5	5	5	5
	Ground glass opacities	3.5	3	2	2	3	3	4	4.5	5	5
	Mucoid impactions	4	3	2	2	3	3	4	5	5	5
	Bronchial wall thickening	4	3	3	3	3.5	4	4.5	5	5	5
						MIN-CT		ID-CT	PN-CT		HR-CT

Table 2: Preclinical image quality assessment. Five-point Likert scale ratings are available for each scan protocol. They indicate image quality compared to the reference, full-dose high-resolution (HR)-CT protocol used in clinical routine (protocol #10). Each value represents the median rating provided by four radiologists. Insufficient lesion delineation is highlighted with orange and red background color (Likert scale: 1-2). Limited but diagnostic lesion delineation is illustrated with lime-green background color (Likert scale: 3). Good image quality (Likert scale: 4) and perfect image quality (Likert scale: 5) are highlighted with dark-green. Grade 4 image quality was used to determine radiation dose cut-offs for HR-CT, pulmonary nodule (PN)-CT (protocol #8), and infectious disease (ID)-CT (protocol #7). Minimum dose (MIN)-CT (protocol #5) reached the lowest dose levels at diagnostic image quality for PN and ID lesions. We subsumed reticulations under the patterns of inter- and intralobular lines.

current-time products (1, 10, 20, 40, 80, 160, 320 mAs). The CTDI$_{vol}$ of the highest protocol with tin prefiltration (3.24 mGy) was 55% lower than the upper dose reference (7.15 mGy). All other settings remained unchanged for all protocols: rotation time, 0.8 seconds; detector collimation, 32 × 0.6 mm (Stellar); simultaneous acquisition of 64 slices by interleaved volume reconstruction; pitch, 0.8. Image reconstruction was performed in thin overlapping slices (1.0 mm; increment, 0.7 mm) using a sharp reconstruction kernel (Br56) and sinogram-affirmed iterative reconstruction at the clinical routine strength level of 3 (minimum strength, 1; maximum strength, 5). The size of the image matrix was 512 × 512 pixels.

Four radiologists subjectively evaluated the images of the human cadaver's chest. Despite not having known lung pathologies, several subclinical pulmonary lesions were present (see Table 2). We decided to acquire IQ ratings of 4 radiologists because the preclinical data were subsequently translated to clinical routine examination protocols. A large data set of ratings is expected to diminish the risk of unprecise IQ ratings. The radiologists had <1, 4, 5, and >10 years of experience in chest CT. The upper reference protocol was used as a standard reference (#10). In consensus, the readers identified 15 pathologic changes in the standard reference and categorized them into 3 different groups: (1) HR lung structures, mainly comprising changes of fibrotic or emphysematous changes; (2) PNs, mainly comprising changes of metastatic disease; and (3) infectious disease (ID), comprising consolidations, ground-glass opacities, and pathologies of the bronchi. The detailed pulmonary patterns that we considered for each group are described in Table 2.

All low-dose protocols (#1–9) were evaluated without knowledge of the acquisition mode but in the knowledge of the pathologic changes. To assess diagnostic acceptability of the low-dose examinations, overall IQ was rated on a 5-point Likert scale (1, nondiagnostic; 2, limited diagnostic; 3, diagnostic with uncertainties; 4, fully diagnostic; 5, perfect). Delineation of the 15 pathologic changes within the lung tissue was rated separately (1, not visible; 2, only visible in the knowledge of image number and position; 3, poor delineation; 4, good delineation; 5, perfect delineation). Character, image number, and position were noted for each of the 15 lesions in the cadaver during the evaluation of the upper reference dose level. All other image series (#1–9) were then evaluated in the knowledge of this lesion catalog but blinded to the acquisition mode. Likert scores ≥4 were considered suitable for optimal reading; Likert scores ≤2 were considered nondiagnostic. Likert score 3 was considered as minimum diagnostic. We calculated contrast-to-noise (CNR) and dose-normalized contrast-to-noise ratio (CNRD) values for each protocol. The body donor signed a declaration of last will in lifetime, which provided consent for research and educational purposes.

Clinical Evaluation

After evaluating the ex-ante trial IQ, the protocols with the lowest radiation dose for optimal IQ (Likert ≥4) were selected for the subgroups PN and ID (Table 2). A protocol with the minimum radiation dose for maintained diagnostic IQ (MIN-CT, Likert ≥3), excluding HR evaluation, was added for cases with high awareness about radiation dose and prospectively waived comfortable IQ. We prospectively applied HR-, PN-, ID-, and MIN-CT in the clinical routine after installing the new CT system in our department. The full-dose factory protocol (130 kV, 54 ref mAs) was used as HR instead of the protocol from the ex-ante trial upon a recommendation by the vendor. We used 130 kV due to the limited tube capacity and the expectation that, even in patients with higher body weight, subtle fibrotic changes remain visible. A total of 88 consecutive patients with a clinical indication for native chest CT were included (Fig. 1). Written informed consent was obtained from each individual. The responsible radiologists assigned the different study protocols under consideration of the individual clinical indication. Clinical indications for HR-CT at our institution were autoimmune disease, which are known to cause lung fibrosis (eg, systemic sclerosis, rheumatic disease, sarcoidosis), the suspicion of silicosis, medication-induced fibrosis, and idiopathic fibrotic disease. Clinical indication for PN-CT was confirmed for dedicated control examinations of 1 or several lung nodules in patients with and without malignant disease. We indicated ID-CT when the distribution, the pattern, and potential complications of pneumonia were critical for further treatment. This was the case for fungal pneumonia and other opportunistic infections in immunocompromised patients, for viral or bacterial pneumonia with severe illness or increasing symptoms under therapy, and before bronchoscopy for patients on intensive care unit. We used MIN-CT for the following indications: 1) patients at a younger age and the suspicion of infectious disease; 2) younger patients with malignancies; 3) follow-up examinations of lung lesions; 4) for patients with high awareness about radiation dose and mild but chronic pulmonary symptoms. The selection algorithm was defined to consistently cover the most critical expected structures from the admission request. So, for example, a patient with a new onset of fever and history of fibrosis would have been selected for HR-CT. Patients who refused to participate in the study, children, and emergency patients were excluded. The study was approved by the local ethical review board and complied with the Declaration of Helsinki. Two radiologists with 5 and >10 years of experience in lung imaging evaluated overall IQ in the same way as in the ex-ante trial. Unlike to the preclinical study part, we decided to perform the IQ rating with only 2 readers because we
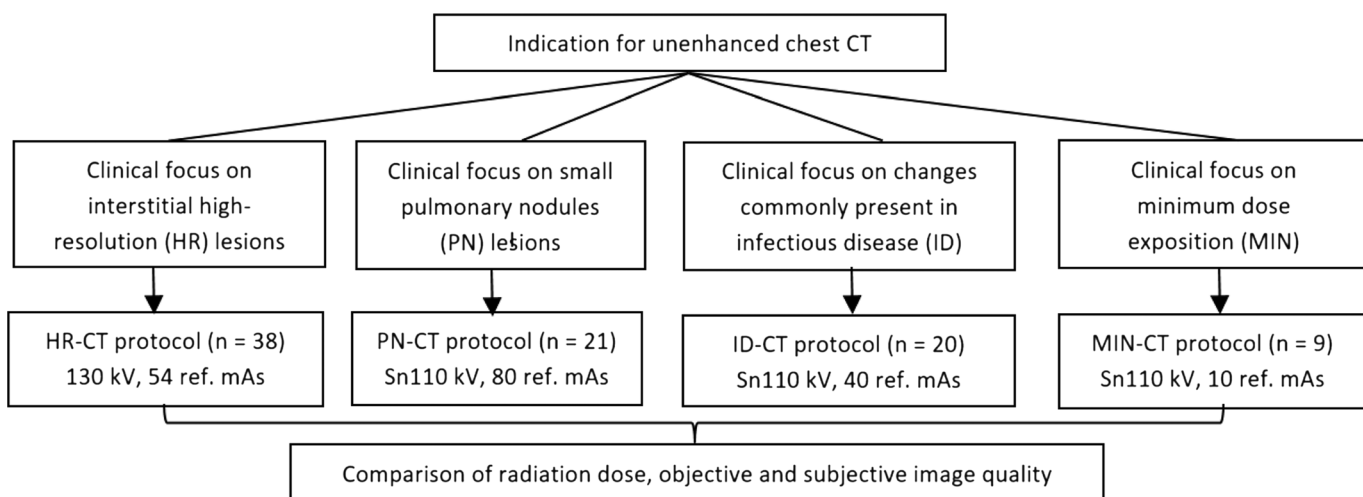

FIGURE 1. Clinical study protocol.

were convinced that the complex and variable in vivo lung disease patterns should be evaluated by readers with the most experience (5 and >10 years) to maintain high reliability. If present, HR structures, PN, and ID lesions were evaluated for each patient on a modified Likert scale (1, unevaluable; 2, uncertain delineation; 3, limited but diagnostic delineation; 4, good delineation; 5, perfect delineation). Objective IQ was assessed as the contrast-to-noise ratio (CNR) following equation 1:

$$CNR = \frac{mean\ attenuation\ (lung) - mean\ attenuation\ (extracorporeal\ air)}{noise\ (extracorporeal\ air)}$$

Equation 1

Dose-normalized contrast-to-noise ratio was calculated following equation 2:

$$CNRD = \frac{mean\ attenuation\ (lung) - mean\ attenuation\ (extracorporeal\ air)}{noise\ (extracorporeal\ air)\ x\sqrt{CTDI}}$$

Equation 2

Radiation Dose

Radiation dose was assessed as $CTDI_{vol}$, dose length product (DLP), and effective dose (ED). Effective dose was calculated using the published k-factor for chest CT ($k = 0.014$ mSv/mGy·cm) as recommended in the literature.[24]

$$ED = DLP \cdot 0.014\ [mSv \cdot mGyx^{-1} \cdot cmx^{-1}].$$

Equation 3

Statistical Analysis

Four experienced radiologists performed the preclinical lesion rating on a 5-point Likert scale. The most experienced radiologists with 5 and >10 years of experience performed the clinical lesion rating also on a 5-point Likert scale.
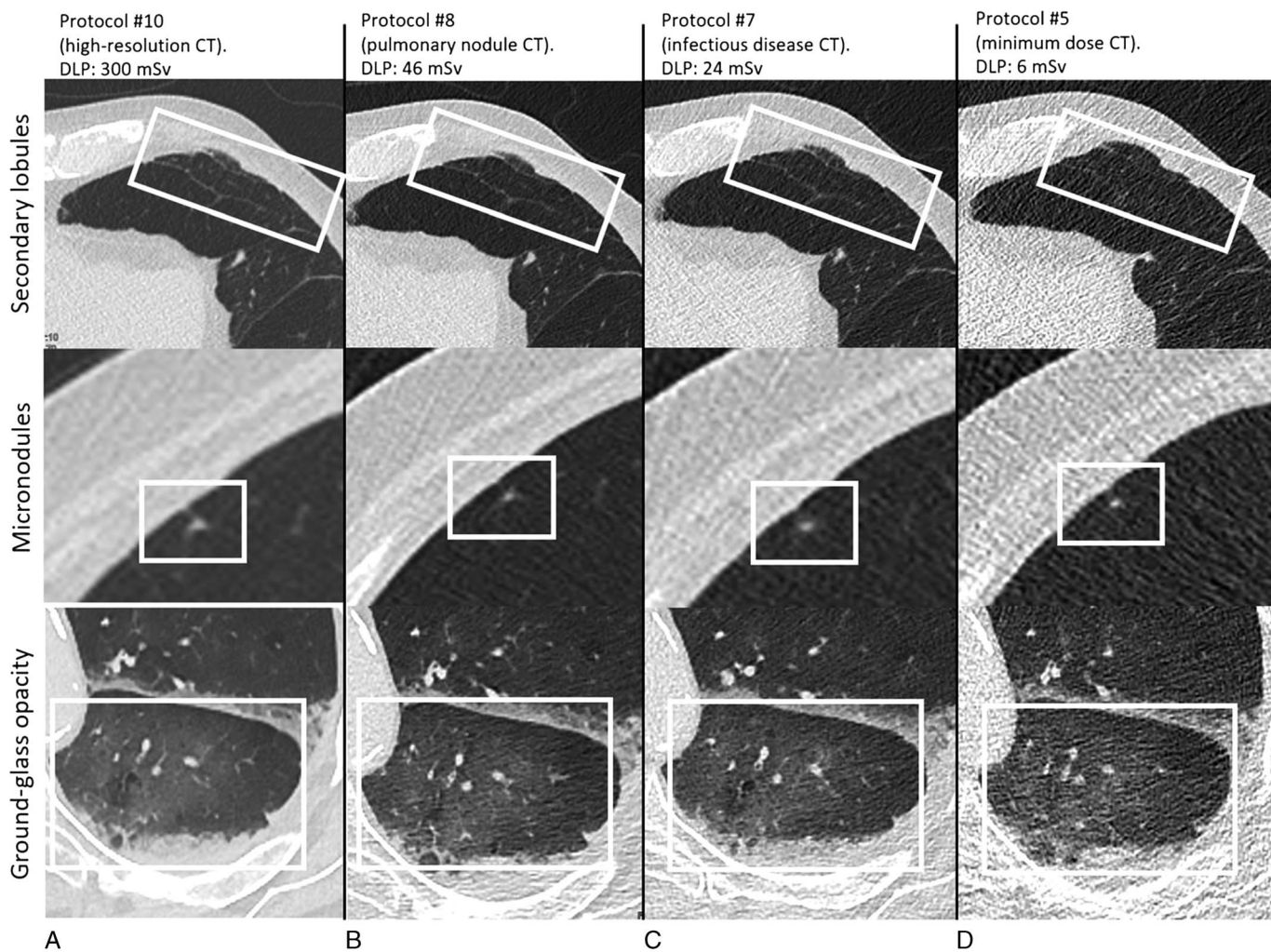

FIGURE 2. Preclinical evaluation of secondary lobules, micronodules, and ground-glass opacity. The radiation dose decreases from protocol A to D. A, Examination protocol #10, dose length product (DLP) = 300, delineation of all structures in perfect quality. B, Examination protocol #8, DLP = 46. C, Examination protocol #7, DLP = 24. D, protocol #5, DLP = 6. We decided to use the following examination protocols in clinical routine for specific indications under consideration of the clinical focus. A, Detection of high-resolution structures (HR-CT). B, detection of pulmonary nodules (PN-CT). C, Detection of infectious diseases (ID-CT). D, Pulmonary imaging at minimum diagnostic radiation dose (MIN-CT). Images were viewed with standard lung window settings (width, 1700; center, −600).

Values are provided as mean and standard deviation in case of normal distribution. Median and interquartile range are shown when normal distribution was not assumed. We used the nonparametric Kruskal-Wallis test with post hoc Dunn-Bonferroni analysis for unrelated samples to compare subjective IQ among the 4 protocols. To compare unrelated samples, we assessed the homogeneity of variances using the Levene test. We applied 1-way analysis of variance with post hoc analysis of Bonferroni (CNRD calculations) or Games-Howell when the data were not homogeneous (CTDI, DLP, and ED calculations). Interrater agreement was assessed by estimating Cohen κ coefficients. We calculated κ coefficients for the complete study and separate values for each study group. Kappa values ≥0.41 were interpreted as moderate, κ values ≥0.61 as substantial, and κ-values ≥0.81 as almost perfect agreement according to Landis and Koch.[25] Intrareader reliability was calculated with intraclass correlation coefficients (ICCs) for reader 1 (R1) and reader 2 (R2). We calculated ICC based on mean ratings, absolute agreement, and a 2-way mixed model. Statistical significance was accepted for P values below a defined significance level of $P = 0.05$. Statistical analysis was performed using the software package SPSS Statistics version 21 (SPSS Inc/IBM, Chicago, IL).

RESULTS

Ex-Ante Trial

All 15 findings were perfectly represented in the upper reference protocol with the overall IQ of 5 for all parenchymal findings (#10). Intralobular lines dropped from good to limited delineation for protocol #8 (110 kV, tin prefiltration, and 160 ref mAs). All PN and ID findings were rated as good or perfect. High-resolution structures and delineation of noncalcified micronodules were rated as poor or below in protocol #7 (110 kV, tin prefiltration, and 80 ref mAs). In the protocol with 20 ref mAs (#5), secondary lobules and intralobular lines were only visible in the knowledge of image number and position in protocol #10. However, at least poor delineation was conserved for all PN and ID findings (Table 2). Based on these results, protocol #10 was considered suitable for HR evaluation, protocol #8 for PN assessment, and protocol #7 for ID. Protocol #5 was considered as MIN-CT for pulmonary evaluation. Computed tomography protocols with tin prefiltration and below 20 ref mAs showed insufficient delineation of pulmonary lesions and structures. Correspondingly, we see a substantial drop of CNRD values from MIN-CT levels (CNRD = 23.1) to the CT protocols with ref mAs below 20 (#4, CNRD = 14.4; #3, CNRD = 15.8; #2, CNRD = 18.2). Figure 2 provides an overview of the IQ of the 4 protocols with subsequent usage in clinical routine.

Clinical Evaluation

The mean age of the 88 patients (male, 68.2%; female, 31.8%) was 60 ± 17 years. HR-CT was selected for 38 patients, PN-CT for 21 patients, ID-CT for 20 patients, and MIN-CT for 9 patients. Consequently, for 57% (total n = 50) of our study patients, reduced radiation dose settings were applicable. CTDI$_{vol}$, DLP, and ED differed significantly among HR-CT, PN-CT, ID-CT, and MIN-CT protocols ($P_{CTDIvol} < 0.001$, $P_{DLP} < 0.001$, $P_{ED} < 0.001$). Post hoc tests were significant (all P's < 0.001), except for ED and CTDI values between ID-CT and MIN-CT ($P = 0.668$ and 0.262). A graphical overview is provided for CTDI$_{vol}$ in Figure 3. The radiation dose of the clinically used HR protocol was one fourth below the HR protocol from the ex-ante trial (#10) but still two thirds above the highest radiation dose with spectral shaping (#9). Respective ED was 2.73 ± 0.41 mSv for HR, 0.64 ± 0.21 mSv for PN, 0.33 ± 0.15 mSv for ID, and 0.15 ± 0.03 mSv for MIN-CT. In the 38 HR-CT examinations, HR structures were present in 100%, PN in 73.7%, and ID lesions in 57.9% of all cases. In the PN protocols, HR structures were present in 95.2%, PN in 61.9%, and ID lesions in 47.6%. In comparison, respective numbers in the ID
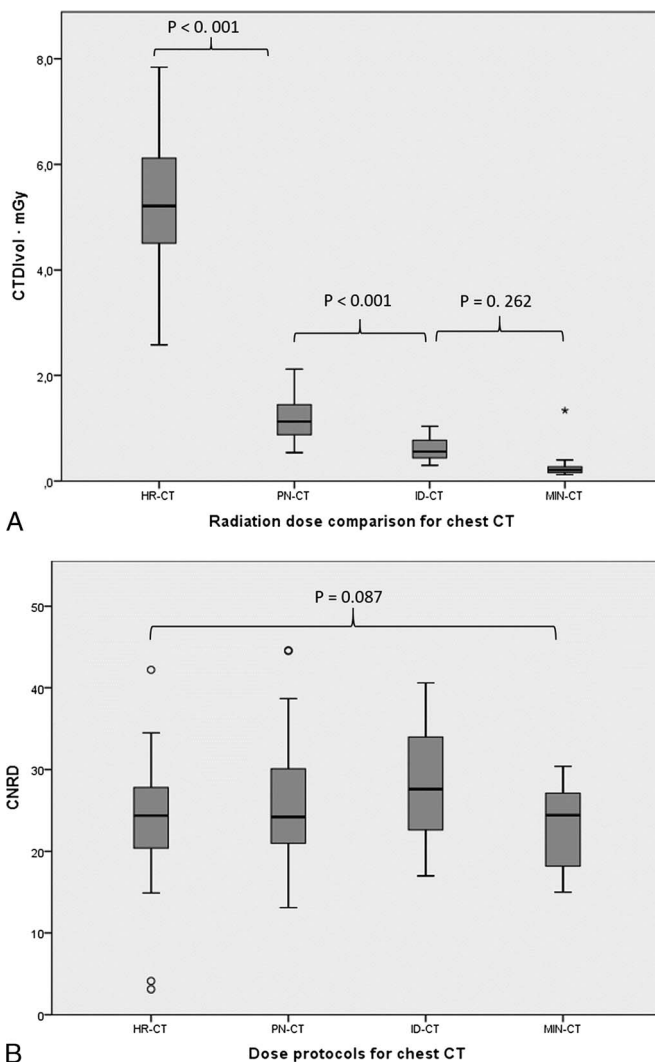

FIGURE 3. Comparison of (A) volume CT dose index (CTDI$_{vol}$) and (B) dose-normalized contrast to noise ratio (CNRD) for personalized examination protocols tailored to clinical indication: High-resolution (HR) CT, pulmonary nodule (PN) CT, infectious disease (ID) CT, and minimum dose (MIN) CT. Boxplot and whisker diagram: boxes show medians, first-quartile, and third-quartile boarders. Whiskers display the minimum and maximum values within 1.5 times the interquartile range. Outliers are marked as asterisk.

examinations were 100% for HR structures, 63.1% for PN, and 47.3% for ID lesions. In the MIN-CT examinations, HR structures were present in 88.9%, PN in 66.7%, and ID lesions in 55.6% of all cases.

Overall IQ differed significantly among the 4 protocols ($P < 0.001$). The differences between HR-CT and PN-CT ($P < 0.001$) as well as between ID-CT and MIN-CT ($P < 0.001$) were statistically significant. Differences in overall IQ between PN-CT and ID-CT were nonsignificant, but PN-CT (median, 4.5; quartiles, 4.0–5.0) tended to be better than ID-CT (median, 4.3; quartiles, 4.0–4.6). Details are shown in Figure 4A and Table 3.

Delineation of HR structures was significantly different in the 4 protocols ($P < 0.001$). Best results with only good or perfect delineation were found for HR-CT, which were significantly better than the other protocols (all P's < 0.001). Representation of the HR structures was limited in a few cases with the PN-CT and ID-CT without statistically significant differences between each other ($P = 1.000$). MIN-CT provided
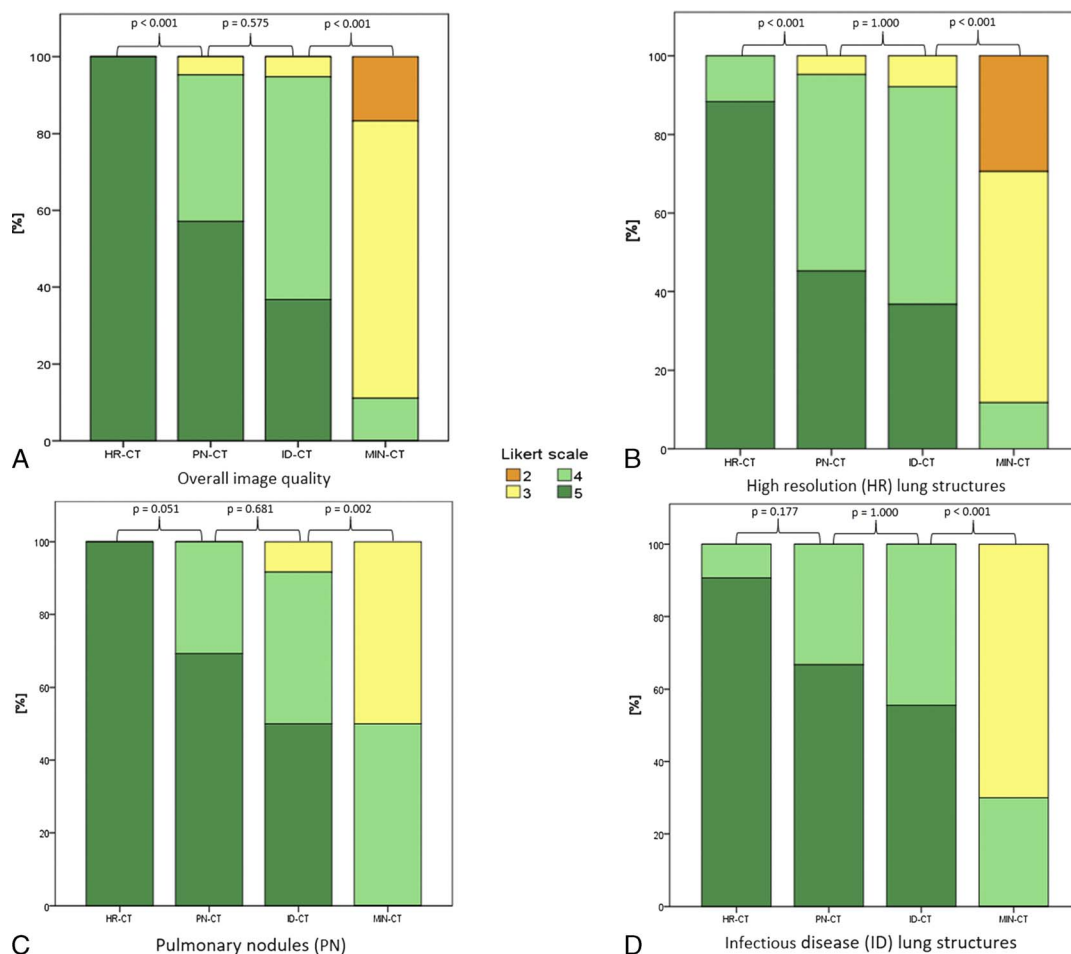
FIGURE 4. A, Comparison of overall image quality. B, Image quality of high-resolution (HR) lung structures. C, Pulmonary nodules (PN). D, Infectious lung disease. Image quality was rated on a 5-point Likert scale (1, unevaluable; 2, uncertain delineation; 3, limited but diagnostic delineation; 4, good delineation; 5, perfect delineation).

limited or uncertain IQ for HR structures in most cases and was significantly worse than the other protocols (all *P*'s < 0.001, Fig. 4B).

Delineation of PN lesions differed significantly among the 4 protocols (*P* < 0.001). Both HR-CT and PN-CT yielded good or perfect lesions delineation (*P* = 0.051). Some cases from ID-CT provided limited delineation of small PNs. Differences were nonsignificant compared with PN-CT (*P* = 0.681) but significant compared with the HR-CT (*P* = 0.002). Pulmonary nodule delineation was limited in most cases with the MIN-CT protocol, which was significantly worse than ID-CT (all *P*'s < 0.002, Fig. 4C).

Delineation of ID lesions differed significantly among the 4 protocols (*P* = 0.001). All lesions evaluated with HR-CT, PN-CT, and ID-CT were rated good or perfect. The highest ranks were found for the HR-CT, which were nonsignificant compared with PN-CT and ID-CT (*P* = 0.177 and *P* = 0.127). The majority of ID lesions in MIN-CT had a limited and significantly worse delineation compared with ID-CT (*P* = 0.001, Fig. 4D and Table 3). However, no PN and no ID lesion was completely unevaluable in the MIN-CT.

Overall interrater correlation was moderate for the clinical evaluation (κ = 0.47). We performed separate calculation of interrater correlation for (1) HR-CT (κ = 0.41), (2) PN-CT (κ = 0.44), (3) ID-CT (κ = 0.46), and (4) MIN-CT (κ = 0.51). Intrareader reliability of both readers showed sufficient values for HR-CT (ICC R1, 0.724; R2,

1.000), for PN-CT (ICC R1, 0.971; R2, 0.930), ID-CT (ICC R1, 0.869; R2, 0.897), and MIN-CT (ICC R1, 0.869; R2, 0.949).

Dose-normalized contrast-to-noise ratio was comparable among all 4 protocols (*P* = 0.087; Fig. 3 and Table 3). Post hoc analysis of Bonferroni showed no significant differences among HR-CT/PN-CT (*P* = 1.000), PN-CT/ID-CT (*P* = 1.000), and ID-CT/MIN-CT (*P* = 0.186) (Fig. 5).

DISCUSSION

Our quadruple radiation dose comparison study proves that personalized CT protocols with minimum radiation dose exposure tailored to the individual clinical indication are feasible. For more than 50% of our patients, personalized protocols with reduced radiation doses were applicable. The radiation dose can be substantially reduced when spectral-shaping techniques are implemented. Pulmonary nodule and ID lesions were detectable with a dose reduction of up 95% in MIN-CT (ED, 0.15 mSv) compared with HR-CT (ED, 2.73), although sharp delineation is limited with this lowest clinically acceptable radiation dose. Our findings are in line with other studies, which show that ultra–low-dose examination protocols with an ED similar to a chest radiograph in 2 planes (MIN-CT) are feasible to detect or control relevant PNs, pneumonia, or genetic diseases.[13,26–29]

TABLE 3. Dose Settings and Image Quality Ratings of Personalized CT Examination Protocols

Protocol	n	kV	ref mAs	CNR	CNRD	CTDI$_{vol}$, mGy · cm	DLP, mGy · cm	ED, mSv	Overall Image Quality	HR Findings	PN Findings	ID Findings
HR-CT	38	130	54	56.6 ± 9.2	25.1 ± 5.7	5.4 ± 1.4	195.1 ± 54.4	2.73 ± 0.4	5.0 (5.0–5.0)	5.0 (5.0–5.0)	5.0 (5.0–5.0)	5.0 (5.0–5.0)
PN-CT	21	Sn110	80	27.1 ± 4.6	26.5 ± 4.6	1.2 ± 0.4	45.6 ± 16.1	0.64 ± 0.2	4.5 (4.0–5.0)	4.5 (4.0–4.5)	5.0 (4.3–5.0)	4.5 (4.5–5.0)
ID-CT	20	Sn110	40	20.9 ± 2.3	28.0 ± 6.7	0.6 ± 0.2	24.4 ± 9.0	0.33 ± 0.05	4.3 (4.0–4.6)	4.0 (3.6–4.5)	4.5 (3.8–5.0)	4.5 (4.3–4.75)
MIN-CT	9	Sn110	10	10.1 ± 1.1	22.8 ± 5.5	0.2 ± 0.1	7.3 ± 1.9	0.15 ± 0.03	2.5 (2.0–2.6)	3.0 (2.5–3.1)	3.0 (2.9–3.8)	3.0 (2.5–3.75)

For radiation dose and CNRD values, mean and standard deviation are given. Median values of image quality ratings are given with an interquartile range.

CT, computed tomography; CNR, contrast-to-noise ratio; CNRD, dose-normalized contrast-to-noise ratio; CTDI$_{vol}$, volumetric CT dose index; DLP, dose length product; ED, effective dose; HR, high-resolution; PN, pulmonary nodule; ID, infectious disease; MIN, minimum dose.

The dedicated ID-CT (ED, 0.33 mSv) has been developed to detect pneumonia and is routinely used in the COVID-19 pandemic in our department. It reaches up to 87% dose reduction compared with the conventional full-dose HR-CT. Pulmonary nodules can be sufficiently detected with the dedicated PN-CT (ED, 0.64 mSv), and a dose reduction up to 77% compared with the full-dose reference protocol is
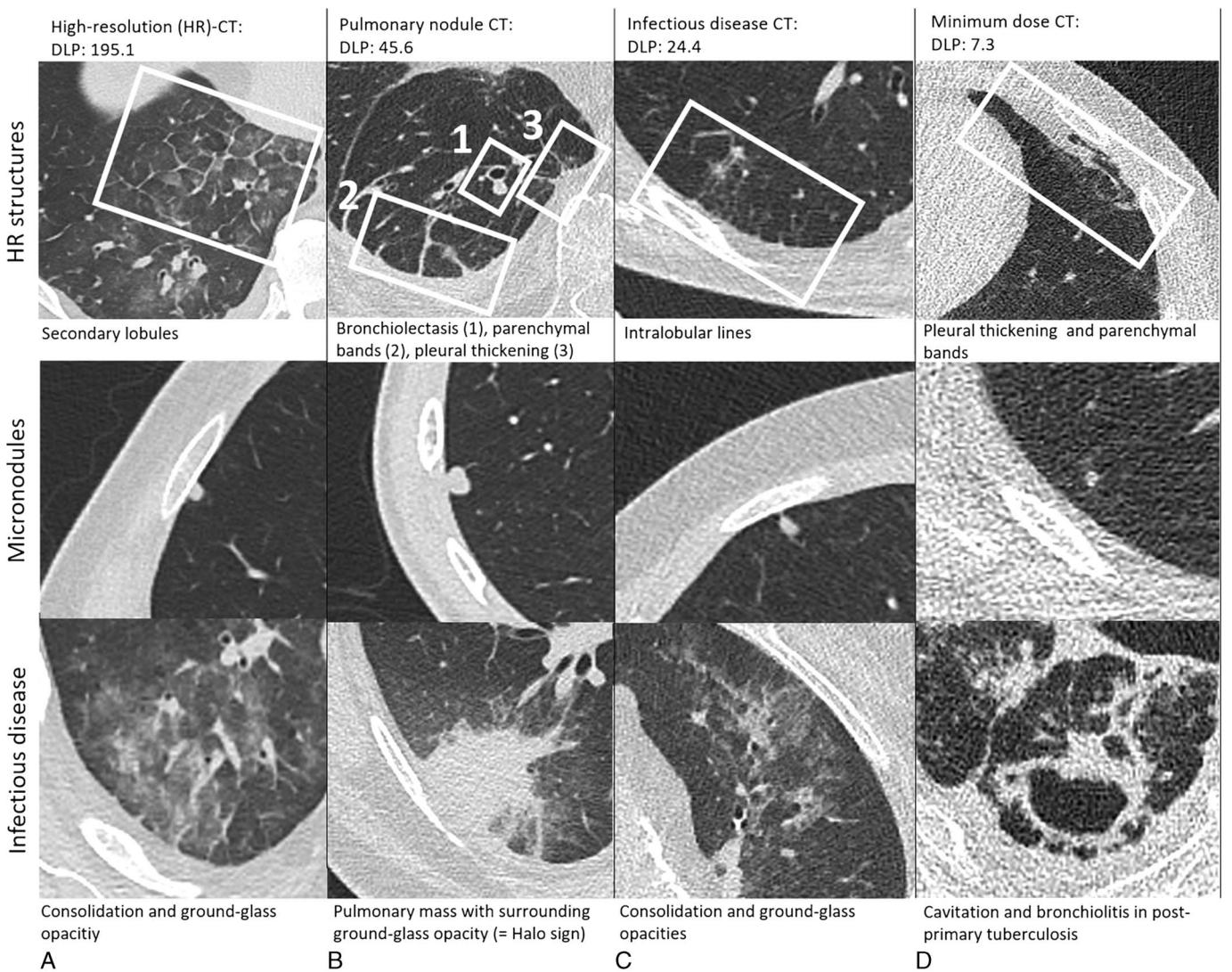

FIGURE 5. Image quality comparison of different dose protocols: (A) high-resolution (HR) CT, (B) PN-CT, (C) ID-CT, and (D) MIN-CT. Examples of different categories of lesions are illustrated for each radiation dose group. Optimal and very good image quality for HR lesions is achievable with protocols A and B. Protocol C provides borderline image quality for HR lesions. In contrast, D provides mainly blurry HR lesions, which are not suitable for adequate lesion evaluation. The micronodules in protocols C and D are increasingly blurry, whereas protocols A and B provide sharp lesion delineation. Infectious diseases are detectable with all CT protocols, but the sufficient characterization of ground-glass opacities is not recommended with MIN-CT. Images were viewed with standard lung window settings (width, 1700; center, −600).

reached. The evaluation of fibrotic changes and other subtle interstitial lesions of the lung parenchyma is reserved to the HR-CT protocol with >2 mSv effective radiation dose.

The reported dose reduction with tin prefiltration of up to 90% is in line with some prior studies, which described comparable radiation dose reduction rates of 80% for calcium scoring[30] and 70% for paranasal sinus CT[5,22] due to spectral shaping. Also, spectral shaping was considered to allow for substantial radiation dose reduction for adult chest CT in phantom studies.[6] However, Messerli et al[13] found that the sensitivity for small PN detection decreases to 91% at ultra–low-dose levels with tin prefiltration (0.13 mSv) compared with 100% in the reference protocol (1.8 mSv) in a study design with intraindividual double exposure. Other studies analyzed the influence of advanced iterative model reconstructions compared with hybrid iterative reconstructions to detect PNs. Especially, micronodules below 4 mm were more frequently detected with the advanced algorithm at 0.67 mSv.[31] Neroladaki et al[32] evaluated the use of model-based iterative reconstructions. They found long reconstruction times but minimum ED values of 0.16 mSv for ultra–low-dose chest CT and 100% sensitivity for lung nodule detection compared with a standard dose CT with an ED of 11.2 mSv.[32]

In contrast to these studies, we aimed to determine and compare the performance of different incremental radiation dose levels for the most frequent clinical indications of unenhanced chest CT. Three different dose levels can be used, taking the individual indications of HR structures, PNs, and ID into account. Furthermore, our results address the need for reliable evaluation, what level of radiation dose is appropriate to detect pneumonia in the context of the COVID-19 pandemic.[33] Several studies describe the findings and importance of chest CT for COVID-19 pneumonia.[2,3,9] The International Atomic Energy Agency reported $CTDI_{vol}$ values for ID-CT in this context from 54 international health care sites in 28 countries (7–11 mGy). The personalized radiation dose level in our study was 95% below this worldwide reference.[34] Other authors recommend a low-dose CT protocol with a comparably low ED of 0.2 mSv to detect COVID-19 pneumonia.[32] However, several further studies describe the benefits of chest CT beyond the COVID-19 pandemic. Upchurch et al[35] report about CT pneumonia, which is not visible on a chest radiograph. However, they state that these patients need the same treatment principles.[35] Nemoto et al[36] describe significant advantages of chest CT in community-acquired pneumonia with poor physical status or chronic heart failure.

Furthermore, Garin et al[37] discuss that chest CT can reduce overdiagnosis of community-acquired pneumonia and helps to identify alternative diagnoses. These studies mentioned previously underline the importance of chest CT to diagnose pneumonia. Therefore, we believe that there is a high need for dose optimization in CT of ID, because an increasing number of CT examination worldwide is expected.

Furthermore, several studies evaluated the appropriateness of various CT examination protocols for lung cancer screening. The National Lung Screening Trial Research Team proved a relative reduction in mortality from lung cancer with low-dose CT screening of 20.0% with average ED levels of 1.5 mSv.[15] Becker et al[38] describe a maximum radiation dose exposure of 1.6 to 2 mSv in the German Lung Cancer Screening Intervention Trial.

Also, de Koning et al[39] found that lung cancer mortality was significantly lower among those who underwent volume CT screening. However, the radiation dose for this trial is not reported. Martini et al[29] reported that sensitivity for nodule detection was only moderate (71%–81%) with a radiation dose equivalent to conventional radiography. Another study from Martini et al[40] with submillisievert chest CT (0.13 mSv) reports substantial interreader variability of nodule measurement. This study did not evaluate lesion detection. This study should contribute to a discussion about the lowest necessary radiation exposure for lung cancer screening because the present results indicate that sufficient nodule delineation is possible with an ED of 0.6 mSv (PN-CT). However,

MIN-CT is leading to blurry lesion margins and reduced delineation. This may complicate accurate measurements necessary for correct categorization of nodules considering Lung-RADS.[41–43]

Limitations

First, the preclinical cadaver examination was conducted on only one cadaver due to ethical concerns. Therefore, not every pulmonary lesion or anatomic structure is entirely representative of other lungs. Second, we used vendor-specific examination protocols with spectral shaping (tin-prefiltration). Consequently, the same radiation dose settings cannot be transferred entirely to other scanners. Third, the size of the 4 study groups was rather small and varied due to a variable amount of clinical indications. Especially, specific clinical indications for MIN-CT were relatively rare. Fourth, although only trained radiologists performed the lesion scoring, we know the potential impreciseness of subjective Likert scale ratings. Also, we know there can always be an overlap of CT indications und imaging patterns when fibrosis, nodules, and pneumonia are evaluated. Fifth, intraindividual comparison of pulmonary lesions was not performed, and comparison of pulmonary lesions over time may be influenced by physiologic changes of IDs or different depths of inspiration. Sixth, we experienced no cases where the IQ was insufficient for the specific clinical indication, and no CT scan had to be repeated. However, our results underline that fibrotic lung disease should not be evaluated with low-dose CT protocols. Seventh, due to the relatively small sample size, future studies should focus on enrolling more patients. Lastly, due to the 5-point Likert scale, we experienced several cases in each study group with differences of 1 Likert scale level (4 vs 5, 3 vs 4), which lead to relatively moderate κ values of interreader agreement. The discriminatory power between nearby Likert ranks still remains subjective. This effect contributed to the moderate κ values in this study.

CONCLUSIONS

The use of personalized chest CT protocols tailored to individual clinical indications leads to significant dose reduction without reducing interpretability. In addition, this study suggests an optimized CT protocol for detecting pneumonia and PNs. MIN-CT allows to control or exclude pulmonary pathologies at dose levels comparable to a chest radiograph in 2 planes.

REFERENCES

1. Guan WJ, Ni ZY, Hu Y, et al. Clinical characteristics of coronavirus disease 2019 in China. *N Engl J Med*. 2020;382:1708–1720.
2. Li K, Wu J, Wu F, et al. The clinical and chest CT features associated with severe and critical COVID-19 pneumonia. *Invest Radiol*. 2020;55:327–331.
3. Wu J, Wu X, Zeng W, et al. Chest CT findings in patients with coronavirus disease 2019 and its relationship with clinical features. *Invest Radiol*. 2020;55:257–261.
4. Hammond E, Chan KS, Ames JC, et al. Impact of advanced detector technology and iterative reconstruction on low-dose quantitative assessment of lung computed tomography density in a biological lung model. *Med Phys*. 2018. doi:10.1002/mp.13057.
5. May MS, Brand M, Lell MM, et al. Radiation dose reduction in parasinus CT by spectral shaping. *Neuroradiology*. 2017;59:169–176.
6. Suntharalingam S, Allmendinger T, Blex S, et al. Spectral beam shaping in unenhanced chest CT examinations: a phantom study on dose reduction and image quality. *Acad Radiol*. 2018;25:153–158.
7. Newell JD Jr., Fuld MK, Allmendinger T, et al. Very low-dose (0.15 mGy) chest CT protocols using the COPDGene 2 test object and a third-generation dual-source CT scanner with corresponding third-generation iterative reconstruction software. *Invest Radiol*. 2015;50:40–45.
8. Saltybaeva N, Martini K, Frauenfelder T, et al. Organ dose and attributable cancer risk in lung cancer screening with low-dose computed tomography. *PLoS One*. 2016;11:e0155722.
9. Lyu P, Liu X, Zhang R, et al. The performance of chest CT in evaluating the clinical severity of COVID-19 pneumonia: identifying critical cases based on CT characteristics. *Invest Radiol*. 2020;55:412–421.

10. Khawaja RD, Singh S, Madan R, et al. Ultra low-dose chest CT using filtered back projection: comparison of 80-, 100- and 120 kVp protocols in a prospective randomized study. *Eur J Radiol*. 2014;83:1934–1944.

11. Gordic S, Morsbach F, Schmidt B, et al. Ultralow-dose chest computed tomography for pulmonary nodule detection: first performance evaluation of single energy scanning with spectral shaping. *Invest Radiol*. 2014;49:465–473.

12. Eberhard M, Stocker D, Milanese G, et al. Volumetric assessment of solid pulmonary nodules on ultralow-dose CT: a phantom study. *J Thorac Dis*. 2019;11:3515–3524.

13. Messerli M, Kluckert T, Knitel M, et al. Ultralow dose CT for pulmonary nodule detection with chest x-ray equivalent dose—a prospective intra-individual comparative study. *Eur Radiol*. 2017;27:3290–3299.

14. Vonder M, Dorrius MD, Vliegenthart R. Latest CT technologies in lung cancer screening: protocols and radiation dose reduction. *Transl Lung Cancer Res*. 2021;10:1154–1164.

15. National Lung Screening Trial Research TeamAberle DR, Adams AM, Berg CD, et al. Reduced lung-cancer mortality with low-dose computed tomographic screening. *N Engl J Med*. 2011;365:395–409.

16. Huber A, Landau J, Ebner L, et al. Performance of ultralow-dose CT with iterative reconstruction in lung cancer screening: limiting radiation exposure to the equivalent of conventional chest x-ray imaging. *Eur Radiol*. 2016;26:3643–3652.

17. Vardhanabhuti V, Pang CL, Tenant S, et al. Prospective intra-individual comparison of standard dose versus reduced-dose thoracic CT using hybrid and pure iterative reconstruction in a follow-up cohort of pulmonary nodules—effect of detectability of pulmonary nodules with lowering dose based on nodule size, type and body mass index. *Eur J Radiol*. 2017;91:130–141.

18. Xu X, Sui X, Song L, et al. Feasibility of low-dose CT with spectral shaping and third-generation iterative reconstruction in evaluating interstitial lung diseases associated with connective tissue disease: an intra-individual comparison study. *Eur Radiol*. 2019;29:4529–4537.

19. Loeve M, Lequin MH, de Bruijne M, et al. Cystic fibrosis: are volumetric ultra-low-dose expiratory CT scans sufficient for monitoring related lung disease? *Radiology*. 2009;253:223–229.

20. Wendel F, Jenett M, Geib A, et al. Low-dose CT in neutropenic patients with fever of unknown origin. *Rofo*. 2005;177:1424–1429.

21. Agostini A, Floridi C, Borgheresi A, et al. Proposal of a low-dose, long-pitch, dual-source chest CT protocol on third-generation dual-source CT using a tin filter for spectral shaping at 100 kVp for coronavirus disease 2019 (COVID-19) patients: a feasibility study. *Radiol Med*. 2020;125:365–373.

22. Wuest W, May M, Saake M, et al. Low-dose CT of the paranasal sinuses: minimizing x-ray exposure with spectral shaping. *Eur Radiol*. 2016;26:4155–4161.

23. Mathieu KB, Ai H, Fox PS, et al. Radiation dose reduction for CT lung cancer screening using ASIR and MBIR: a phantom study. *J Appl Clin Med Phys*. 2014;15:4515.

24. Deak PD, Smal Y, Kalender WA. Multisection CT protocols: sex- and age-specific conversion factors used to determine effective dose from dose-length product. *Radiology*. 2010;257:158–166.

25. Landis JR, Koch GG. The measurement of observer agreement for categorical data. *Biometrics*. 1977;33:159–174.

26. Kim Y, Kim YK, Lee BE, et al. Ultra-low-dose CT of the thorax using iterative reconstruction: evaluation of image quality and radiation dose reduction. *AJR Am J Roentgenol*. 2015;204:1197–1202.

27. Hu-Wang E, Schuzer JL, Rollison S, et al. Chest CT scan at radiation dose of a posteroanterior and lateral chest radiograph series: a proof of principle in lymphangioleiomyomatosis. *Chest*. 2019;155:528–533.

28. Kroft LJM, van der Velden L, Giron IH, et al. Added value of ultra-low-dose computed tomography, dose equivalent to chest x-ray radiography, for diagnosing chest pathology. *J Thorac Imaging*. 2019;34:179–186.

29. Martini K, Barth BK, Nguyen-Kim TD, et al. Evaluation of pulmonary nodules and infection on chest CT with radiation dose equivalent to chest radiography: prospective intra-individual comparison study to standard dose CT. *Eur J Radiol*. 2016;85:360–365.

30. Tesche C, De Cecco CN, Schoepf UJ, et al. CT coronary calcium scoring with tin filtration using iterative beam-hardening calcium correction reconstruction. *Eur J Radiol*. 2017;91:29–34.

31. Zhang M, Qi W, Sun Y, et al. Screening for lung cancer using sub-millisievert chest CT with iterative reconstruction algorithm: image quality and nodule detectability. *Br J Radiol*. 2018;91:20170658.

32. Neroladaki A, Botsikas D, Boudabbous S, et al. Computed tomography of the chest with model-based iterative reconstruction using a radiation exposure similar to chest x-ray examination: preliminary observations. *Eur Radiol*. 2013;23:360–366.

33. Lee C. Managing radiation dose from chest CT in COVID-19 patients. *Radiology*. 2020:204129.

34. Homayounieh F, Holmberg O, Al Umairi R, et al. Variations in CT utilization, protocols, and radiation doses in COVID-19 pneumonia: results from 28 countries in the IAEA study. *Radiology*. 2021;298:E141–E151.

35. Upchurch CP, Grijalva CG, Wunderink RG, et al. Community-acquired pneumonia visualized on CT scans but not chest radiographs: pathogens, severity, and clinical outcomes. *Chest*. 2018;153:601–610.

36. Nemoto M, Nakashima K, Noma S, et al. Prognostic value of chest computed tomography in community-acquired pneumonia patients. *ERJ Open Res*. 2020;6:00079–02020.

37. Garin N, Marti C, Scheffler M, et al. Computed tomography scan contribution to the diagnosis of community-acquired pneumonia. *Curr Opin Pulm Med*. 2019;25:242–248.

38. Becker N, Motsch E, Gross ML, et al. Randomized study on early detection of lung cancer with MSCT in Germany: study design and results of the first screening round. *J Cancer Res Clin Oncol*. 2012;138:1475–1486.

39. de Koning HJ, van der Aalst CM, de Jong PA, et al. Reduced lung-cancer mortality with volume CT screening in a randomized trial. *N Engl J Med*. 2020;382:503–513.

40. Martini K, Ottilinger T, Serrallach B, et al. Lung cancer screening with submillisievert chest CT: potential pitfalls of pulmonary findings in different readers with various experience levels. *Eur J Radiol*. 2019;121:108720.

41. Martin MD, Kanne JP, Broderick LS, et al. Lung-RADS: pushing the limits. *Radiographics*. 2017;37:1975–1993.

42. Chelala L, Hossain R, Kazerooni EA, et al. Lung-RADS version 1.1: challenges and a look ahead, from the AJR Special Series on Radiology Reporting and Data Systems. *AJR Am J Roentgenol*. 2021;216:1411–1422.

43. Kastner J, Hossain R, Jeudy J, et al. Lung-RADS version 1.0 versus Lung-RADS version 1.1: comparison of categories using nodules from the national lung screening trial. *Radiology*. 2021;300:199–206.